Numerical Investigation of Plasma Dynamics in Cal Poly's Electrical Propulsion Vacuum Facilities

Anthony J. Presto *, David C. Tennant †, and Lubos Brieda‡
California Polytechnic State University of San Luis Obispo, San Luis Obispo, California, 93407, USA

This paper presents current efforts to develop numerical simulation capability to complement Cal Poly Aero Department's research into electric propulsion (EP). The department provides students with access to a 6-foot by 10-foot 'STELLA' thermal vacuum chamber, which can be converted to a 14-foot-long EP-testing configuration. Additionally, students have access to numerous smaller chambers, including a 'Big Green' bell-jar. These facilities are used for testing electric propulsion prototypes and to study facility effects. Such effects are especially of concern to Hall Effect Thrusters, which can ingest backscattering plume particles due to their open design. The primary effort utilizes the development of CAD models of these two facilities, models for a gridded ion thruster and a Hall thruster, corresponding surface meshes, and existing plasma thruster modeling code to produce predictions of plume densities, pressures, and temperature when considering the inclusion and exclusion of facility effects. As part of future work, representative experimental probe measurements will be obtained, which will be used to validate the simulations.

I. Nomenclatture

HET	=	Hall effect thruster
GIT	=	Gridded Ion Thruster
EP	=	Electric Propulsion
Xe	=	Xenon Gas
Xe^+	=	Ionized Xenon Gas
H	=	HET Annulus Height
L	=	HET Annulus Length
R	=	Annulus Radius
$\vec{B}$	=	Magnetic Field Vector
$\vec{E}$	=	Electric Field Vector
$CTSP$	=	Contamination Transport Simulation Program

II. Introduction

Hall effect thrusters and gridded ion thrusters are increasingly important to spacecraft mission architectures requiring efficient, low-thrust orbital maneuvers and station keeping. Relative to chemical propulsion, electric propulsion devices provide substantially higher specific impulse, enabling reduced propellant mass for a given total impulse and thereby increasing delivered payload or mission margin. Continued development of EP technologies relies on ground testing in vacuum facilities. However, measurements obtained in chambers can differ from in-space behavior due to facility-specific boundary conditions, including elevated background neutral density, nearby material surfaces, and facility-dependent electrical return paths. These influences, referred to as facility effects, are particularly relevant to HETs since their open geometry can ingest background neutrals, and plume–surface interactions can increase charge-exchange populations, modifying diagnostic signatures [1–3].

Cal Poly's Aerospace Engineering Department supports electric propulsion research with multiple vacuum facilities, including the 'STELLA' thermal vacuum chamber (nominally 6ft by 10ft and configurable to an extended EP-testing

*Graduate Student, Aerospace Engineering Department, Cal Poly San Luis Obispo, AIAA Student Member 1551322
†Undergraduate Student, Aerospace Engineering Department, Cal Poly San Luis Obispo, AIAA Student Member, 1869228
‡Assistant Professor, Aerospace Engineering Department, Cal Poly San Luis Obispo, Senior Member 211732, lbrieda@calpoly.edu

layout) and a smaller bell-jar facility known as 'Big Green'. In the present work, two representative test articles are considered: an SPT-100 HET operated in STELLA and a 15 cm-class GIT evaluated in Big Green. Although these devices differ in discharge physics and plume characteristics, both can be analyzed using numerical modeling methodology to quantify plume evolution and wall interactions.

This paper documents the development of a simulation workflow intended to be repeatable and accessible for laboratory use and future student projects. The workflow consists of CAD development of facility and test-article geometries, generation of grouped surface meshes representing physically meaningful regions, and application of an existing particle transport code to propagate macroparticles through the chamber environment and recover macroscopic quantities such as number density and pressure from particle statistics. Consistent with the present scope, the numerical analysis employed here does not resolve charged-particle dynamics. Instead, the thruster exhaust is represented through parametric outlet populations, including a primary directed population and an additional slower population intended to capture the chamber-scale influence of slow, charge-exchange-like particles on transport trends. For the STELLA configuration, the beam dump and pump boundaries are modeled as strong sinks via low-temperature surface assignments to better represent effective particle removal in those regions.

Preliminary simulations demonstrate chamber-scale plume expansion and interaction with internal boundaries, yielding macroscopic density fields that reflect confinement by the facility geometry and approach a statistically steady distribution under fixed source and boundary assumptions. These results motivate a structured facility-effects validation plan based on representative chamber probe measurements.

Section III of this paper summarizes facility-effect mechanisms relevant to HET ground testing and motivates the modeling approach. Section IV describes the modeled facilities and test articles, as well as the CAD modeling. Section V describes the software used for meshing, as well as the techniques implemented to ensure accurate modeling and geometry groupings. This details the surface meshing, including boundary group definitions and mesh parameter selections. Section VI provides an overview of the code used for numerical modeling and its suitability for facility-scale particle transport on CAD-derived surface meshes. Additionally, this section describes the setup involved to ensure this code accurately reflects the facility effects by the HET in STELLA and the GIT in Big Green. Sections VII-VIII present the facility-effect metrics, validation plan, results, and sensitivity considerations, followed by conclusions and future work in Sections IX-X.

III. Facility-Effects Background

Electric propulsion thrusters are routinely characterized in ground-based vacuum facilities. However, finite chamber size, pumping capacity, and material boundary conditions can perturb thruster operation and plume properties compared to standard operating conditions. These differences are referred to as facility effects and are especially important for HETs because their open geometry can ingest surrounding particles and interact with nearby chamber hardware, visible in Fig. 1. Literature reviews emphasize that elevated background pressure can influence measured performance and that any testing comparisons require careful control and consistent definitions of pressure and facility configuration [1].

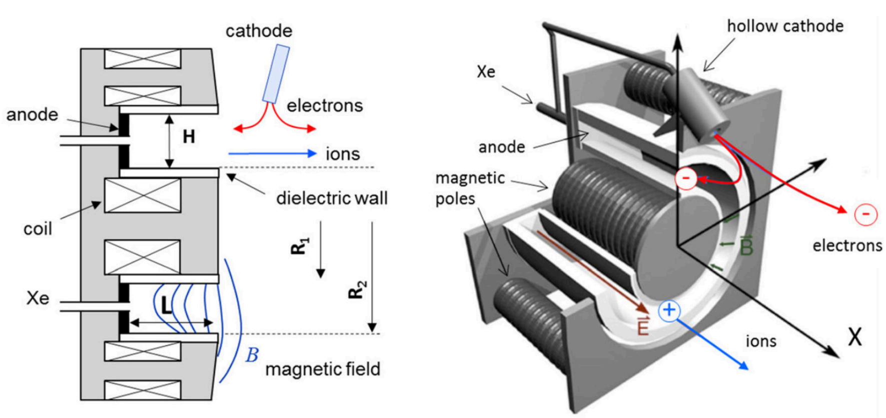

Fig. 1 SPT-100 Diagram Depicting Open Annulus & Operations [4]

A. Operational Meaning of Facility Effects

In this paper, facility effects refer to changes in either thruster operation, plume properties, or diagnostic measurements that arise due to the test environment rather than the thruster alone. The mechanisms most relevant to this study are

- **Back-Pressure and Background Neutral Ingestion:** Finite pumping increases background neutral density compared to space. HETs can ingest this gas, and these ingested particles could be ionized and accelerated, altering plume behavior and thrust. Pumping-speed variation studies provide methods to quantify back-pressure sensitivity [5].
- **Charge-Exchange Frequency:** Higher neutral densities from wall interactions increase the charge-exchange probability, producing slower ions that widen the plume and can contribute to more particles returning to the thruster and facility surfaces. Experimental studies have documented these pressure-dependent plume properties [6].
- **Plume-Wall Interactions:** Facility walls and beam dumps intercept ions and can sputter material that deposits elsewhere. Back-sputtering modeling in HET test facilities demonstrates that these effects can be significant in ground testing [2].
- **Electrical Boundary Conditions:** Grounded hardware and return paths can influence plume potential. For example, plume diagnostics such as Faraday probes can be pressure-sensitive. Recommended practices and design considerations are documented by Walker and Brown [3, 7].

B. Prior Approaches and Motivation

Experimental approaches typically vary vacuum chamber pressure, subsequently measuring thrust, discharge current, and plume signatures to determine facility sensitivity. One common approach for isolating facility effects on back-pressure or ingestion is varying pumping speed [5]. Numerical approaches range from PIC models to DSMC neutral transport and vacuum chamber integrated plume simulations. Since facility effects often depend strongly on geometry, this work emphasizes the efforts towards CAD modeling and meshing to quantify trends in temperature, number density, and pressure relative to chamber scale.

IV. Geometry & CAD

This study focuses on two Cal Poly Aero Department EP test facilities: the STELLA thermal vacuum chamber in an EP-testing configuration and the Big Green bell-jar chamber. The modeled test articles include a simplified SPT-100 HET and a gridded ion thruster, each represented as a surface geometry suitable for surface-based particle transport.

A. STELLA

STELLA is a 6-ft-by-10-ft thermal vacuum chamber that can be converted to an approximately 14-ft long EP-testing configuration for housing an SPT-100 like the one in Fig. 2. For this work, the modeled STELLA EP configuration includes the main chamber, thruster chamber, and chamber door (see Fig 3a). Internally, a thruster mount is used to support the SPT-100, as well as a beam dump to redirect the plume (Fig. 3b).

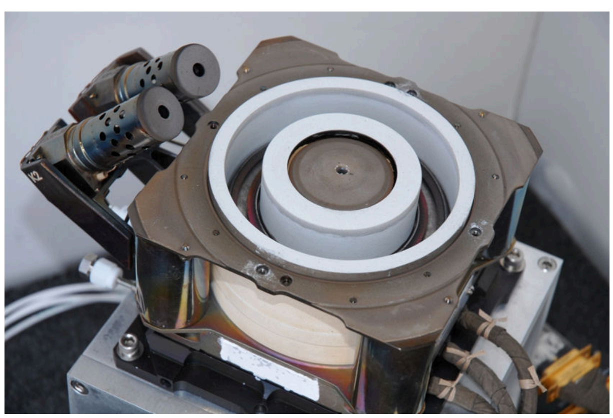

Fig. 2 SPT-100 Hall Effect Thruster Physical Model [8]

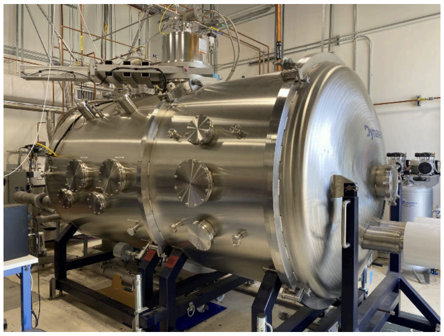

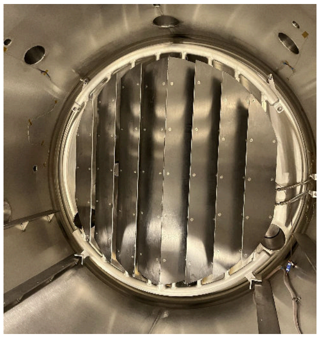

(a) STELLA Vacuum Chamber Shell **(b) STELLA Beam Dump**

Fig. 3 STELLA Vacuum Chamber & Beam Dump in EP-Testing Configuration

CAD modeling efforts focused on capturing the aspects of these geometries that would have the greatest impact on facility effects, with external surface modeling serving to provide analogous visuals. This allowed confidence in the numerical results while simplifying the subsequent mesh relative to the full geometry. For this paper, the primary STELLA model contained the STP-100, thruster mount, and beam dump (Fig. 4a, 4b, and 4c). However, an additional model was made to showcase the thermal shroud and platen, which will be used in future work (see Fig. 5a, 5b, and 5c). A watertight meshing configuration was generated by unioning the shell parts, dump, and mount into a single clean body suitable for robust surface meshing and particle-surface intersection.

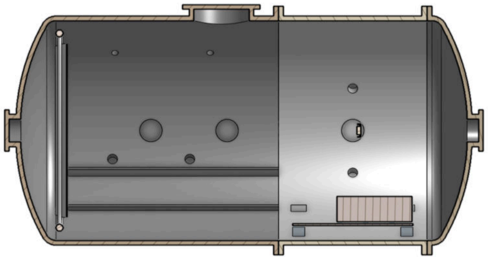

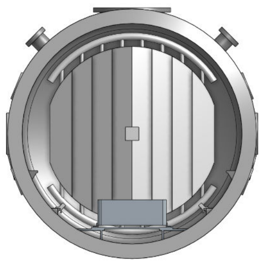

(a) Cross-Section Side View **(b) Open-Chamber Front View**

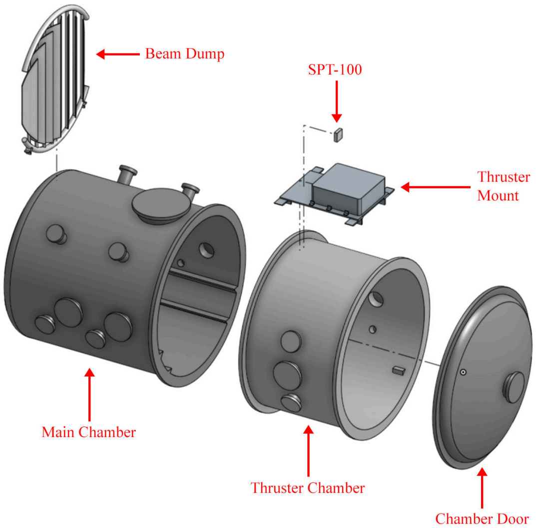

(c) Exploded & Labeled Isometric View

Fig. 4 STELLA CAD Model with Beam Dump in EP-Testing Configuration

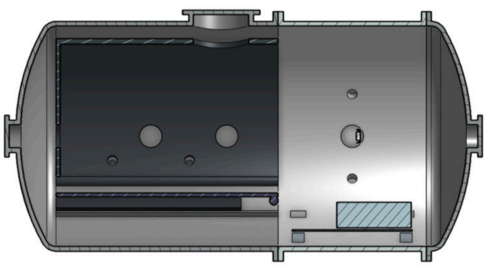

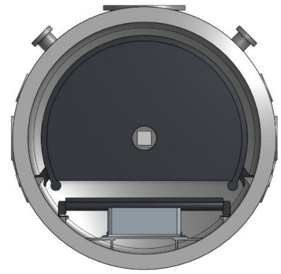

(a) Cross-Section Side View **(b) Open-Chamber Front View**

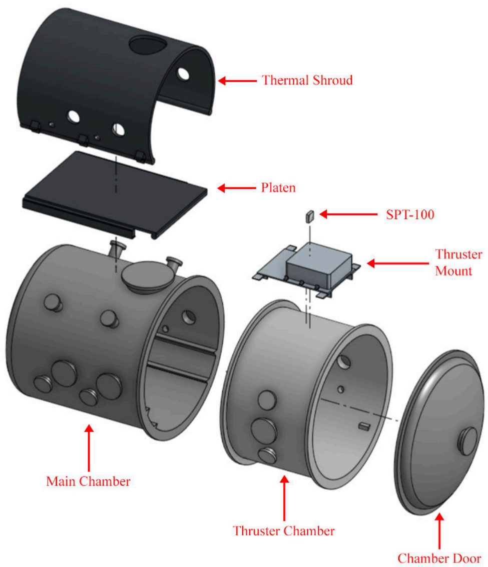

(c) Exploded & Labeled Isometric View

Fig. 5 STELLA CAD Model with Thermal Shroud & Platen in EP-Testing Configuration

B. Big Green

Big green is a bell-jar-style vacuum chamber that can house a variety of thrusters (Fig. 6a). Due to a lack of historical documentation, measurements were taken manually for both Big Green and the GIT (Fig. 6b). The chamber was drawn in two separate parts and assembled via SolidWorks along with the GIT. The assembly is representative of how the bell jar chamber functions. Small and detailed geometries were later simplified to streamline surface meshing and improve quality metrics (see Fig. 7).

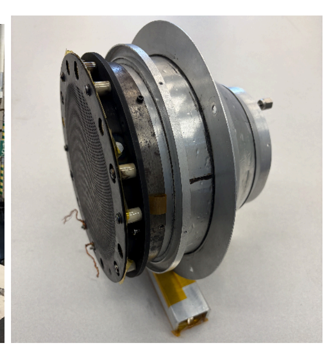

(a) Chamber **(b) GIT**

Fig. 6 Big Green Vacuum Chamber & 15cm Gridded Ion Thruster

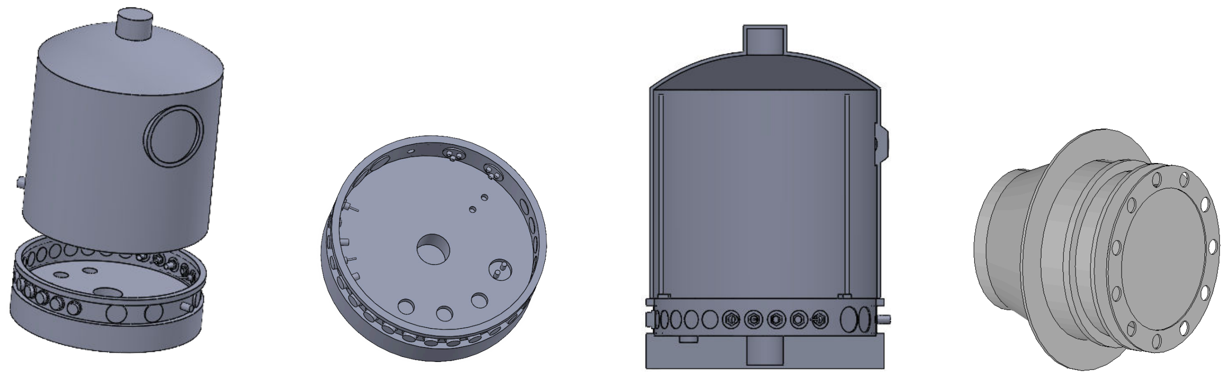

(a) Exploded assembly **(b) Collar** **(c) Section View** **(d) GIT CAD**

Fig. 7 Big Green Vacuum Chamber and GIT CAD

V. Mesh Generation

Surface meshes were generated in the open-source software SALOME and the mesh generator NETGEN 2D, allowing multi-algorithm mesh generation. Groups of faces were created from the surface geometry based on different sets of hypotheses that filter for desired criteria, such as coplanar faces. This allowed for both of the vacuum chambers to have mesh criteria different from those of their respective thrusters. Grouped mesh regions enabled various geometries and faces to have specified temperatures or be set as a mass flow inlet, crucial to accurately simulating EP and the sticking of particles.

A. STELLA

For creating the STELLA chamber surface mesh, a minimum and maximum cell size of 0.47m and 2.6e-5m were set, respectively. This ensured that mesh coarseness could strategically be generated in areas of less complexity while still capturing fine details for surface interactions in more complex geometric regions. A NETGEN 2D fineness of 'moderate' with a growth rate of 0.3 was set with curvature limiting to preserve mesh orthogonality and skewness. This resulted in a surface mesh of 185232 elements with 84110 nodes for both the STELLA chamber and the SPT-100 (Fig. 8). Note that the surface mesh of the chamber shell is only for the internal surface, as the geometry is watertight, and outside geometry has no effect on the internal particle behavior.

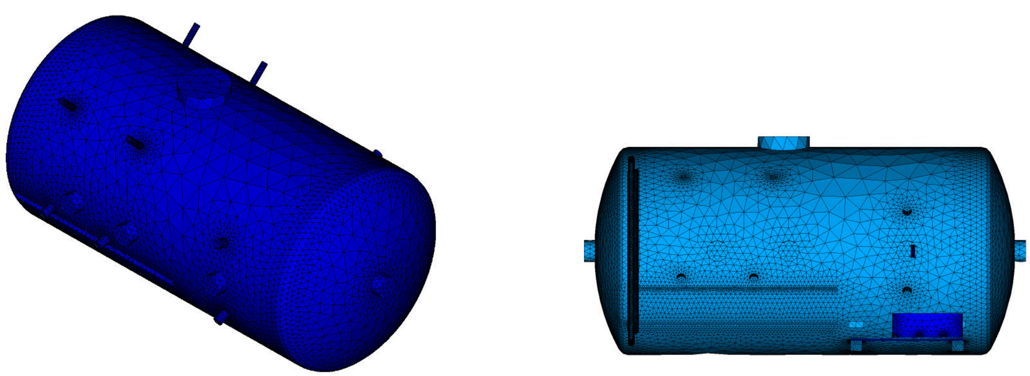

(a) Orthogonal View **(b) Cross-Section Side View**

Fig. 8 STELLA Vacuum Chamber Mesh

For the purpose of accurate numerical modeling, mesh grouping for both the beam dump and the main vacuum pump was needed. This allowed the temperature for both mesh groups to be specified, resulting in more accurate representations of molecular sticking for the respective surfaces (Fig. 9a). For the SPT-100 mesh, a surface grouping was required for the inlet to later be set as a particle source (Fig. 9b).

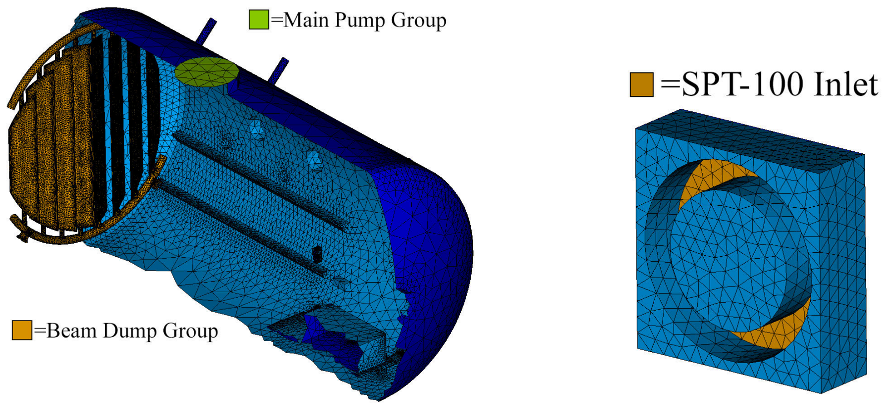

(a) STELLA Chamber Mesh Groupings **(b) SPT-100 Mesh & Grouping**

Fig. 9 STELLA & SPT-100 Mesh Groupings

B. Big Green and GIT

Surface mesh was created for Big Green, and a minimum and maximum cell size of 0.09mm and 6.61mm were set, respectively. This was set to reduce meshing errors in places where the geometry was very fine. This surface mesh resulted in 22206 elements with 10601 nodes (see Fig. 10a and 10b). Groups are classified via coplanar faces and are represented by different colors. A separate mesh for the GIT with a minimum and maximum cell size of 0.05mm and 1.313mm, respectively. This surface mesh resulted in 4144 elements with 1546 nodes (see Fig. 10c). A separate group was necessary for the face plate of the thruster for particles to transport off of.

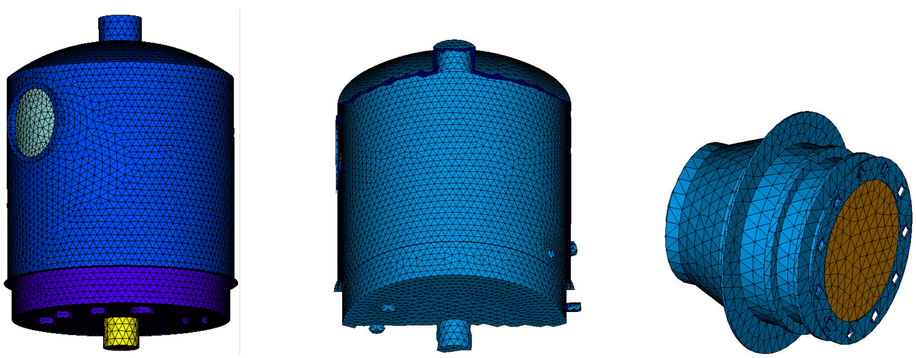

(a) Orthogonal View **(b) Section View** **(c) Gridded Ion Thruster**

Fig. 10 Big Green & GIT Mesh and Groupings

VI. Numerical Modeling Efforts

To simulate facility effects in both vacuum chambers, the 'Contamination Transport Simulation Program' was used. CTSP is a kinetic macroparticle transport code in which many simulation particles are advanced concurrently through discrete time steps, and macroscopic quantities are recovered from particle statistics [9]. Particle velocity is integrated using a fourth-order Runge–Kutta method, and, for common force-free molecular transport cases, particle position is advanced with a forward Euler update [9]. One of the main tasks of this code is detecting particle-surface interactions by having geometric intersection testing at each time step [9]. To avoid unnecessary computational expense, CTSP stores the surface mesh in an internal octree, testing only nearby elements, and uses multithreading for parallel intersection checks. The time-stepping procedure can also resolve multiple surface impacts within one step [9]. Additionally, CTSP does not require a volume mesh for particle transport, making it well-suited for the facility modeling performed in this paper.

A structured sampling grid is specified for macroscopic field visualization and future comparison to probe measurements. To represent facility pumping and particle removal, the surface temperatures for both chamber shells are set to 298K, while both pumps and STELLA's beam dump are set to 0K. The 0K assignment intends to approximate strong collection behavior on these surfaces, as the beam dump negates most particle scattering, and the pumps are meant to remove particles. The propellant for the HET and GIT is xenon and argon gas, respectively, which is emitted by a Maxwellian source to accurately reproduce plume scattering. Since CTSP does not currently support charged particles and their interactions, a secondary, slower Maxwellian source population is defined to approximate charge exchange ions. For numerical stability, the runs are advanced with a time step of 1e-6s for 10,000 time steps. For both facility cases, a simulation is run with all particles sticking for a baseline case without facility effects.

VII. Results

The comparison for both facility cases is restricted to the thermodynamic fields available from the present dataset: static pressure, temperature, and number density. These variables are used to emphasize differences attributable to the presence of the facility environment. The imposed mass flux is kept consistent across cases with respect to each thruster, enabling direct comparisons.

A. STELLA

Figures 11a and 11b show contours of pressure, number density, and temperature for both configurations. In the case with no facility effects (Fig. 11a), particles have no opportunity to return from surfaces and interact with the plume. This is made clear through no particle presence being observed behind the beam dump or the HET's exit plane. For pressure and number density, the facility-enabled case exhibits higher peak values relative to the facility-free case, while the facility-disabled case has a higher peak temperature (Table 2).

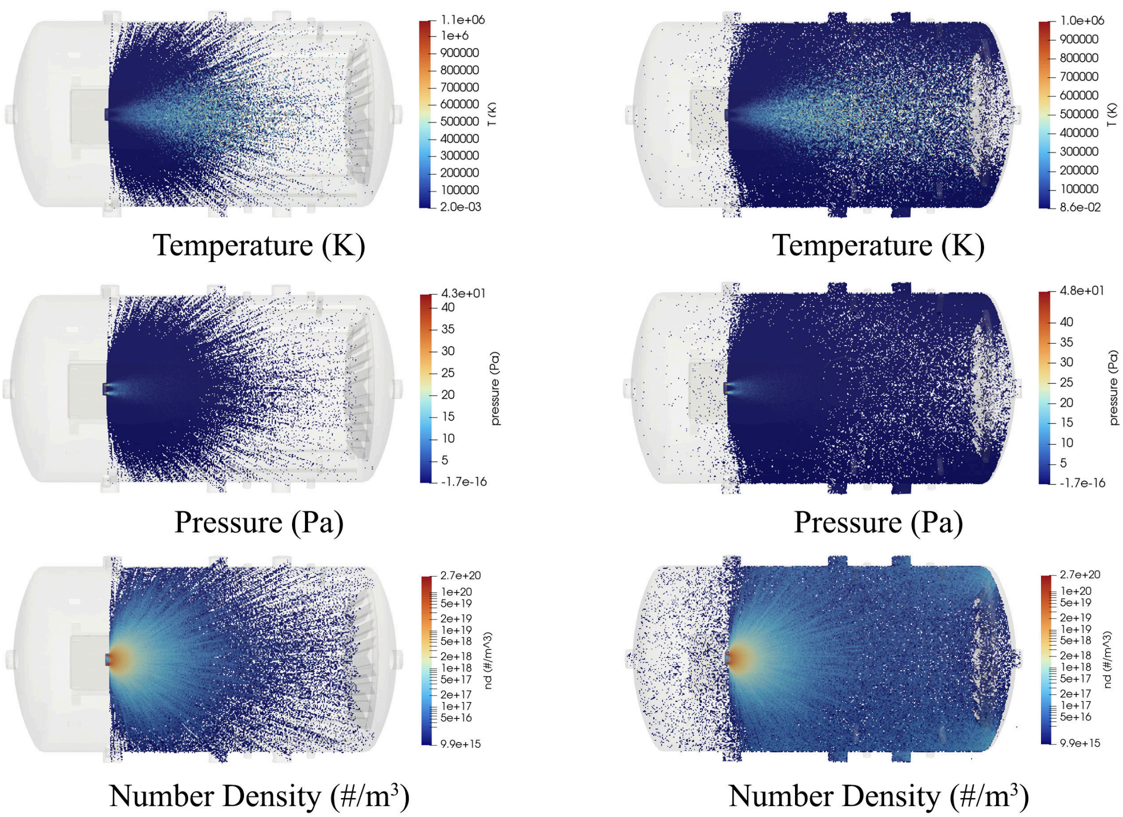

(a) Facility Effects Disabled **(b) Facility Effects Enabled**

Fig. 11 STELLA Chamber & SPT-100 Contours with and without Facility Effects

Table 1 STELLA Peak Plume Properties With & Without Facility Effects

Case	Number Density ($\#/m^3$)	Pressure (Pa)	Temperature (K)
Facility Effects Disabled	2.671e+20	43.16	1.092e+06
Facility Effects Enabled	2.678e+20	47.72	9.994e+05

The most pronounced differences occur near the thruster annulus, where increased back-pressure and neutral density are expected to be most influential. In contrast to these variables, the static temperature shows the prominent differences within the central plume. The results indicate that facility effects alter not only the magnitude of the thermal field but also the spatial location of peak temperature.

B. Big Green

Similarly to the aforementioned results, Fig. 12a and 12b compare contours of particle interactions with and without facility effects. It was once again observed that, for pressure and number density, the facility-enabled case exhibited higher peak values than the facility-free case, and the facility-disabled case had a higher peak temperature (Table 2).

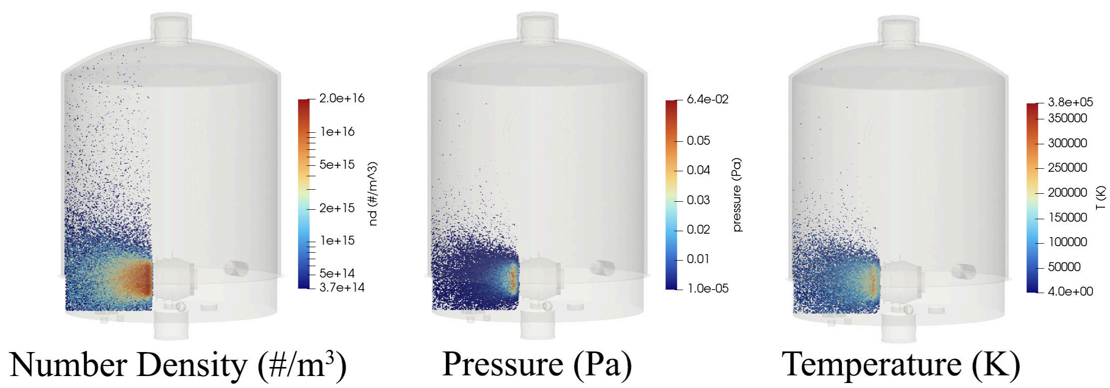

(a) Facility Effects Disabled

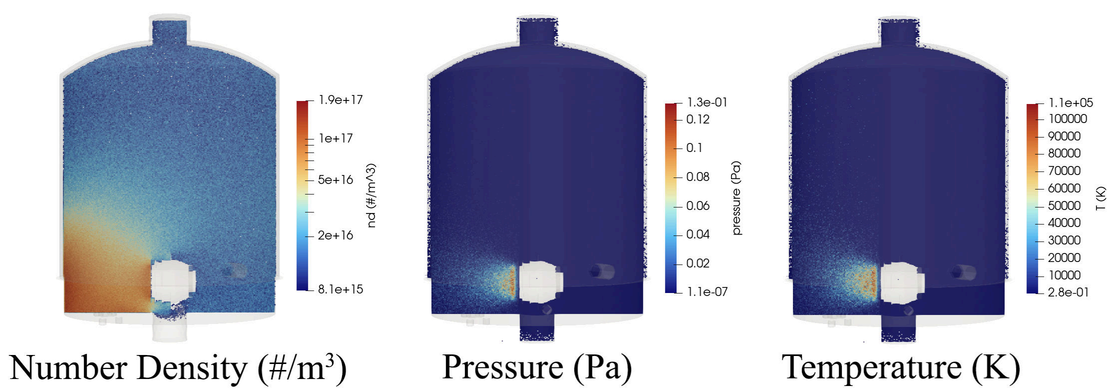

(b) Facility Effects Enabled

Fig. 12 Big Green Chamber & GIT Contours with and without Facility Effects

Table 2 Big Green Peak Plume Properties With & Without Facility Effects

Case	Number Density ($\#/m^3$)	Pressure (Pa)	Temperature (K)
Facility Effects Disabled	2.027e+16	0.0639	3.816e+05
Facility Effects Enabled	1.883e+17	0.1315	1.090e+05

Visible differences occur, as in the HET case, near the thruster exit plane, where facility effects are expected to have the greatest impact on back-pressure and neutral density. Once again, the results indicate that enabling facility effects results in a lower peak static temperature. Since enabling facility effects results in a higher back-pressure and neutral density, there is also an increase in collisions between argon molecules. As high-energy particles are exhausted and collide with the walls, the temperature-determined sticking coefficient results in some of these particles returning to the plume. Having lost their energy due to their residence time on the wall, static temperature in the plume is lowered while number density and pressure increase. This holds for the HET as well as the GIT and sufficiently explains the varying phenomena seen in Fig. 11 and 12.

VIII. Conclusion and Future Work

This paper developed and demonstrated a repeatable numerical workflow for assessing facility effects in Cal Poly's electric propulsion vacuum facilities using representative CAD and surface meshes combined with CTSP particle transport. The STELLA EP-testing configuration and the Big Green bell-jar facility were modeled with grouped surface meshes to represent physically meaningful boundaries, such as the chamber shell, pump surfaces, beam dump, and thruster exit plane, enabling simulation of plume transport and chamber interactions in realistic geometries. A consistent meshing strategy was implemented for both facilities and thrusters to support particle–surface intersection and boundary property assignment.

Comparisons between cases with and without facility effects showed clear facility-dependent trends in both chambers. In both vacuum chambers, enabling facility effects produced increased peak pressure and number density relative to the case without facility effects. The facility-disabled case exhibited a higher peak temperature in both chambers, going against the previous trends. The largest differences were observed near the thruster annulus for STELLA's SPT-100 HET, where back-pressure and neutral density are expected to be most influential. Similar behavior was observed for Big Green and its GIT, where facility-enabled simulations yielded higher peak number density and pressure, along with lower peak temperature, with the most visible differences occurring near the thruster exit plane. Collectively, these results support the central premise that chamber geometry and boundary interactions can measurably alter plume properties and must be considered when testing and interpreting plume environments.

Future work will focus on improving physical fidelity and validating the model against experimental measurements. First, representative probe diagnostics will be used in STELLA and Big Green to compare measured trends against predicted number density and pressure fields and to characterize uncertain boundary interactions. Second, the facility boundary modeling will be refined beyond the present temperature-based sticking coefficient by incorporating more explicit sticking and more realistic pumping representations. Third, the approximate two-population outlet model used to approximate charge-exchange particles will be further examined for accuracy, and future extensions will pursue more physics-based production of slow populations. In pursuit of this accuracy, since CTSP currently does not support ionized species or their interactions, further development will investigate coupling approaches that incorporate externally computed fields or the updating of CTSP's code. This would allow for EP thrusters at Cal Poly's facilities to be modeled with increased confidence, providing future students with the tools needed for academic success.

Acknowledgments

The authors gratefully acknowledge the Cal Poly Aerospace Engineering Department and the College of Engineering at California Polytechnic State University for supporting this independent research. This work was made possible through the assistance of Congressman Salud Carbajal, the Air Force Research Laboratory, and Dynavac in securing funding for and developing STELLA. The donation of an SPT-100 thruster from the Air Force Research Laboratory and a gridded ion thruster from the Jet Propulsion Laboratory further enabled this research, supporting continued electric propulsion efforts for future students. Providing students with opportunities to study electric propulsion advances career development and contributes to the future of spaceflight.

References

[1] Byers, D., and Dankanich, J. W., "A Review of Facility Effects on Hall Effect Thrusters," *The 31st International Electric Propulsion Conference*, September 2009.

[2] 20170000957, N., "Back-sputter modeling for Hall thruster facilities," *NASA Technical Report*, 2017.

[3] Brown, D. L., Walker, M., and Szabo, J. J., "Recommended Practice for Use of Faraday Probes in Electric Propulsion Testing," *Journal of Propulsion and Power*, September 2016. https://doi.org/10.2514/1.B35696.

[4] Boeuf, J.-P., "Tutorial: Physics and modeling of Hall thrusters," *Journal of Applied Physics 121 011101*, January 2017. https://doi.org/10.1063/1.4972269.

[5] Hoffer, R. R., Peterson, P. Y., and Gallimore, A. D., "Characterizing Vacuum Facility Backpressure Effects on the Performance of a Hall Thruster," *The 27th International Electric Propulsion Conference*, October 2001.

[6] 20140017063, N., "Plume/near-field characterization vs background pressure," *NASA Technical Report*, 2014.

[7] Walker, M. L. R., Hoffer, R. R., and Gallimore, A. D., "The Effects of Nude Faraday Probe Design and Vacuum Facility Backpressure on the Measured Ion Current Density Profile of Hall Thruster Plumes," *AIAA 2002-4253*, July 2002. https://doi.org/10.2514/6.2002-4253.

[8] Nakles, M. R., William A. Hargus, J., Delgado, J. J., and Corey, R. L., "A Performance Comparison of Xenon and Krypton Propellant on an SPT-100 Hall Thruster," *AIAA 2012-4116*, August 2012. https://doi.org/10.2514/6.2012-4116.

[9] Brieda, L., "Numerical Model for Molecular and Particulate Contamination Transport," *Journal of Spacecraft and Rockets*, April 2019. https://doi.org/10.2514/1.A34158.